PHYSICAL REVIEW B VOLUME 45, NUMBER 15 15 APRIL 1992-I

Probing localization and mobility of an excess electron in *a*-Si by quantum molecular dynamics

A. Nakano, P. Vashishta, and R. K. Kalia
Concurrent Computing Laboratory for Materials Simulations, Louisiana State University, Baton Rouge, Louisiana 70803-4001
and Department of Physics and Astronomy, Louisiana State University, Baton Rouge, Louisiana 70803-4001

L. H. Yang
Physics/H Division, Lawrence Livermore National Laboratory, P. O. Box 808, Livermore, California 94550
(Received 26 September 1991)

The behavior of an excess electron in *a*-Si is studied over a wide temperature range using the quantum-molecular-dynamics approach. The electron is found to be localized in a nearly spherical void of radius ~ 3 Å, and is surrounded by a ring of eight Si atoms. The simulation results for the electron mobility are in good agreement with the time-of-flight measurements.

I. INTRODUCTION

Photogenerated excess electrons in time-of-flight (TOF) mobility measurements provide very useful insight into the nature of localized states near the conduction band.[1-3] In these experiments the mobility μ is measured from the distance d transversed by excess electrons during transit time t in an external electric field E: $\mu = d/(Et)$. Experiments in *a*-Si indicate that the electron mobility is thermally activated over a temperature range of 150–320 K.[4,5] In the early TOF measurements by Le Comber and Spear, the room-temperature mobility was found to be 0.1 $cm^2/V\,s$ and the activation energy 0.19 eV over the aforementioned temperature range.[6] More recent measurements[3,4] by a number of different groups find the room-temperature mobility to be around 1 $cm^2/V\,s$ and the activation energy to be 0.13 eV.

In the temperature range of 150–320 K, a multiple-trapping model is used to explain the observed thermally activated behavior of the electron mobility.[7-9] Assuming a thermal equilibrium distribution of free carriers and carriers trapped in shallow traps, the extended-state mobility μ_{ext} is reduced relative to μ by the fraction of time that a carrier on the average spends in an extended state. Thus, one finds that

$$\mu = \mu_{ext}\left[1+\frac{g(E_a)}{g(E_c)}\exp(\Delta E/k_B T)\right]^{-1}, \quad (1)$$

where $g(E_c)$ and $g(E_a)$ are the densities of states at the conduction-band mobility edge and trap states, respectively, and $\Delta E = E_c - E_a$ is the activation energy. Widely different values of μ_{ext}, ranging from 10 to 500 $cm^2 V\,s$, have been estimated from Eq. (1).[4]

Very recently, attempts have been made to measure the electron mobility in *a*-Si and *a*-Si:H in the picosecond domain using photoinduced absorption experiments.[10] The picosecond domain is readily accessible to computer simulation and, with the recent development of quantum-molecular-dynamics (QMD) technique,[11-13] mobility simulations on these short time scales can be performed by the same TOF method as used in real experiments.

In this paper, we describe the QMD simulation results concerning the microscopics of localization and mobility of an excess electron in *a*-Si. Three-dimensional visualization shows that the excess electron is trapped in voids whose radii are approximately 3 Å. The mobility of the excess electron is calculated using a subtraction approach based on the difference in the electron dynamics at zero and finite electric fields. This approach yields a good signal-to-noise ratio. The calculated electron mobility is in good agreement with TOF mobility experiments over the whole temperature range between 150 and 300 K. The activation energy is found to be 0.1 eV, which is also in accord with the measured value.

The outline of this paper is as follows. In the next section, we explain the quantum-molecular-dynamics algorithm. Interaction potentials used in the simulations are discussed in Sec. III. In Sec. IV, we describe the numerical procedure, and the results are presented in Sec. V.

II. QUANTUM-MOLECULAR-DYNAMICS ALGORITHM

Let us first consider the situation where the physical system consists of an excess electron interacting with N solicon atoms at a finite temperature T. In the temperature range of interest, i.e., between 150 and 300 K, Si atoms behave as classical particles. The excess electron moves under the influence of a time-dependent potential, $V(\mathbf{r},\{\mathbf{R}_l(t)\})$, that depends on the position of Si atoms, $\{\mathbf{R}_l(t)\}$. The Schrödinger equation for the electron reads

$$i\hbar\frac{\partial}{\partial t}\psi(\mathbf{r},t) = H\psi(\mathbf{r},t), \quad H = -\frac{\hbar^2}{2m}\nabla^2 + V(\mathbf{r},\{\mathbf{R}_l(t)\}), \quad (2)$$

where $\psi(\mathbf{r},t)$ is the excess electron wave function and m is its mass. Formally, one can write the solution of Eq. (2) as

$$\psi(\mathbf{r},t+\Delta t) = T\exp\left[-\frac{i}{\hbar}\int_t^{t+\Delta t} H\,dt'\right]\psi(\mathbf{r},t), \quad (3)$$

 ©1992 The American Physical Society

where T is the time-ordering operator and Δt is a time increment. For sufficiently small Δt (3) can be written as[13]

$$\psi(\mathbf{r},t+\Delta t)=\exp\left[-i\frac{\Delta t}{2\hbar}V(\mathbf{r},t)\right]\exp\left[i\Delta t\frac{\hbar\nabla^2}{2m}\right]\times\exp\left[-i\frac{\Delta t}{2\hbar}V(\mathbf{r},t)\right]\psi(\mathbf{r},t)+O((\Delta t)^3)\ . \tag{4}$$

In the case of bulk systems without any external fields, one can use periodic boundary conditions and implement Eq. (4) with use of discrete fast Fourier transforms. The simulation cell is divided into a regular grid, and at each time interval the wave function $\psi(\mathbf{r},t)$ and the potential $V(\mathbf{r},\{\mathbf{R}_l(t)\})$ are expressed on the grid points. Then there are three steps involved in the execution of Eq. (4).

(i) Matrix multiplication of $\exp[-i\Delta t V(\mathbf{r},\{\mathbf{R}_l(t)\})/2\hbar]$ and $\psi(\mathbf{r},t)$ in the real space. The result $\xi(\mathbf{r})$ is available on the grid points.

(ii) The next operation, $\exp(i\Delta\hbar\nabla^2/2)\xi(\mathbf{r})$, is performed in the momentum space:

$$\exp\left[i\Delta t\frac{\hbar\nabla^2}{2m}\right]\xi(r)=\sum_{\mathbf{k}}\exp\left[-i\Delta t\frac{\hbar k^2}{2m}\right]\zeta(\mathbf{k})e^{i\mathbf{k}\cdot\mathbf{r}}\ . \tag{5}$$

This step involves taking the direct fast Fourier transform of $\xi(\mathbf{r})$, multiplying the Fourier transform $\zeta(\mathbf{k})$ with $\exp(i\Delta t\hbar k^2/2)$, and then taking the inverse discrete fast Fourier transform.

(iii) The last step involves matrix multiplication between $\exp[-i\Delta t V(\mathbf{r},\{\mathbf{R}_l(t)\})/2\hbar]$ and the outcome of step (ii).

Repeated application of these three steps provides the wave function at successive intervals of time.

Together with the propagation of the wave function at each time interval, the positions of classic atoms, $\{\mathbf{R}_l(t)\}$, and the potential $V(\{\mathbf{R}_l(t)\})$ have to be evaluated. The time evolution of $\{\mathbf{R}_l(t)\}$ follows Newton's equations,

$$M\frac{d^2\mathbf{R}_l}{dt^2}=-\nabla_l U(\{\mathbf{R}_l(t)\})-\nabla_l\int d\mathbf{r}\,V(\mathbf{r},\{\mathbf{R}_l(t)\})|\psi(\mathbf{r},t)|^2\ , \tag{6}$$

where M is the mass of a Si atom. The first term on the right-hand side of Eq. (6) arises from the interaction among Si atoms, while the second term is due to the interaction of a Si atom with the excess electron. Equation (6) is valid only if the excess electron is in the lowest-energy state at every instant and nonadiabatic events are absent during the time evolution of the excess electron wave function. The solution of Eq. (6) requires knowledge of the interaction potentials U and V. The form of U and V we have used is discussed in Sec. III.

Recently the excess electron mobility in helium gas[14] and water[15] has been calculated with a straightforward application of the QMD approach outlined above. In these simulations, an external electric field is applied and the average drift velocity along the direction of the applied field is calculated. These mobility simulations are beset with the difficulty that for small external fields the fluctuations in the velocity are much larger than the velocity response to the external field and, as a result, the signal-to-noise ratio is too poor to yield meaningful results. These direct mobility simulations have to be performed at sufficiently high values of the electric field so that the response is above the level of fluctuations. However, too large an electric field can lead to nonadiabatic dynamics for the excess electron.

The problem of poor signal-to-noise ratio is also present in nonequilibrium simulations of classical systems. To alleviate this problem, Ciccotti and Jacucci have developed an approach for classical systems in which equilibrium and nonequilibrium simulations are performed with identical initial conditions.[16] The particle trajectories of equilibrium and nonequilibrium simulations are monitored for a time τ over which the equilibrium and nonequilibrium trajectories are correlated. The response to an external field is calculated by subtracting the equilibrium value of the dynamic variable conjugate to the field from its nonequilibrium value. Since the equilibrium and nonequilibrium values of the dynamical variable are correlated over the time interval τ, the subtraction method eliminates the random fluctuations, leaving behind the systematic response to the external field. Ciccotti and Jacucci have demonstrated that the subtraction method is equivalent to obtaining the response from the time-correlation function of the dynamic variable in an equilibrium simulation. For a charged particle in a Lennard-Jones fluid, the mobility calculated with the subtraction method agrees with the Green-Kubo formula and the simulation results in liquid Ar are also in good agreement with experimental measurements.[16]

The classical subtraction technique has been extended to the case of mixed quantum-classical systems.[17] For an excess electron in a-Si, the Hamiltonian in the presence of an external field, $\mathbf{E}=(E,0,0)$, is

$$\mathcal{H}(t)=\frac{1}{2m}\left[\frac{\hbar}{i}\nabla-eEt\right]^2+V(\mathbf{r},\{\mathbf{R}_l(t)\})\ . \tag{7}$$

The average velocity is calculated from

$$\langle\hat{v}_x(t)\rangle=\mathrm{tr}[e^{-\beta H}\hat{v}_x(t)]=\lim_{t\to\infty}\frac{1}{T}\int_0^T dt_1\langle\psi_0(t_1)|\hat{v}_x(t)|\psi_0(t_1)\rangle, \tag{8}$$

where

$$\hat{v}_x(t)=U^{\dagger}_{\mathcal{H}}(t)\hat{v}_x U_{\mathcal{H}}(t) \tag{9}$$

and $\hat{v}_x=(i\hbar\partial/\partial x-eEt)/m$. In Eq. (8), H and ψ_0 are the electron Hamiltonian and the ground-state wave function, respectively, without the external field; in Eq. (9), $U_{\mathcal{H}}$ is the time-evolution operator in the presence of the field.

In order to remove the large random fluctuations and calculate the systematics of the velocity response to the external field, equilibrium and nonequilibrium simulations are performed for a time τ using identical initial conditions for the wave packet and the configuration of Si atoms. The velocity response, which is the difference in the velocities calculated from the nonequilibrium and

equilibrium simulations over the time interval τ, exhibits a much improved signal-to-noise ratio.

Special attention must be paid to the choice of τ. For classical systems, Ciccotti and Jacucci argue that the total simulation time should be less than the duration over which the equilibrium and nonequilibrium simulations are correlated.[16] In the case of mixed quantum-classical systems where one is interested in the response of quantum particles, finite-size effects may require special attention.[17] For example, when periodic boundary conditions are used, a quasifree particle can diffuse over the entire length L of the box in time $\tau_d \sim L^2/D$, where D is the self-diffusion coefficient of the quantum particle. If the simulation is run longer than τ_d, then spurious phase-coherence effects can mask the real transport of quantum particles. Should such a situation arise, the system size for the nonequilibrium simulation should be increased so that the velocity response can be monitored longer. The asymptotic value of the response can be calculated from these different finite-size simulations.

The subtraction technique has been applied successfully to calculate the mobility of an excess electron in helium gas at 77 K.[17] The QMD simulations were performed over a wide range of helium densities. Over that range both the quasifree and self-trapped behavior for the excess electron are observed. The calculated velocity response of the electron is found to have a good signal-to-noise ratio. The mobility results are in good agreement with the time-of-flight measurements.

III. INTERACTION POTENTIALS

In the present simulations, effective potentials are used to describe the Si-Si atom interaction U and the electron-silicon atom interaction V. U is taken to be the Stillinger-Weber potential:[18] It consists of a two-body potential and a three-body term that takes into account the covalent interactions in the system. Using this potential, MD simulations have been performed for liquid, amorphous, and microclusters of Si. The success of these simulations is well documented. In a-Si MD simulations for the static structure factor and bond-angle distribution are in good agreement with experiments.[19] Simulation results for the phonon density of states in a-Si are also in good agreement with inelastic neutron-scattering measurements.[19]

The interaction between an electron and a silicon atom is described by an effective potential of the form

$$V(r)=\varepsilon_0 \exp[-(r/r_0)^2]\Theta(r/r_c) - (\alpha e^2/2r^4)[1-\Theta(r/r_c)] , \qquad (10)$$

where $\Theta(x)=1-[1-\exp(-x^2)]^6$. The first term represents a repulsive core due to the Pauli principle and Coulomb interaction between the excess electron and the electrons of a silicon atom. The second term is an attractive interaction experienced by the excess electron at large distances due to the electronic polarizability α of silicon atoms.

The parameters ε_0, r_0, and r_c are determined from two separate self-consistent electronic structure calculations in the density-functional formalism.[20] In both calculations, a random network of 54 Si atoms is considered.[21] The first calculation is performed for a system of 54 Si ions and 216 valence electrons, with the electron-ion interaction described by a nonlocal pseudopotential[22] and the electron-electron interaction including the Hartree, exchange, and correlation effects. For the exchange-correlation potential, we use the local-density approximation and the form of the potential is Perdew and Zunger's fit[23] to the exchange-correlation energy results of the Green's-function Monte Carlo calculations.[24] In the second self-consistent electronic structure calculation, the ionic positions are still the same random network configuration of 54 Si atoms as before. In addition to the 216 valence electrons, there is now the additional excess electron and a uniform, neutralizing background. The electron-ion and electron-electron potentials have the same form as in the first calculation.

The purpose of these two calculations is to identify the appropriate length and energy scales for the excess electron in the a-Si network. The difference in the total energies of the two calculations, after suitably subtracting off the contribution of the excess background charge in the second calculation, provides the energy scale for the excess electron. The length scale associated with the excess electron in an a-Si network is estimated from the extent of the excess electron localization, i.e., the participation ratio $[\Omega \int d\mathbf{r} |\varphi_i(\mathbf{r})|^4]^{-1}$, where $\varphi_i(\mathbf{r})$ is the excess electron orbital and Ω is the volume of the 54-atom cell.

Next, MD simulations are performed on an a-Si system in which the atoms interact via the Stillinger-Weber potential U. The amorphous system is obtained by a melt-quench process. Starting with a well-thermalized high-temperature liquid at 5000 K, the system is cooled successively to 4000, 3000, and 2000 K. At each temperature, the system is thermalized for 50 000 MD time steps (one MD time step is equal to 0.605 femtosecond). The 2000-K system is cooled "slowly" to 1500, 1000, 600, and 300 K. Again at each temperature the system is thermalized for a long time. These four systems are well-thermalized glassy states.

In one of the configurations at 300 K, an excess electron is injected. The initial wave function for the excess electron is taken to be a Gaussian. Keeping with positions of Si atoms fixed, the Gaussian wave packet is propagated in imaginary time using the prescription in Eq. (4). A long imaginary-time propagation allows the electron to reach the ground state corresponding to the given configuration of Si atoms. For different amorphous configurations of Si atoms, these long imaginary-time propagations were carried out. The parameters ε_0, r_0, and r_c are chosen so that the ground-state energy of the excess electron and its participation ratio in the ground state agree with the values obtained from the electronic structure calculations. The resulting parameters are $\varepsilon_0=4.49$ eV, $r_0=2.04$ Å, and $r_c=2.25$Å. The value of α is taken to be 5.48×10^{-24} cm^3. The parameters are related to the length of the energy scale of excess electron in a-Si.

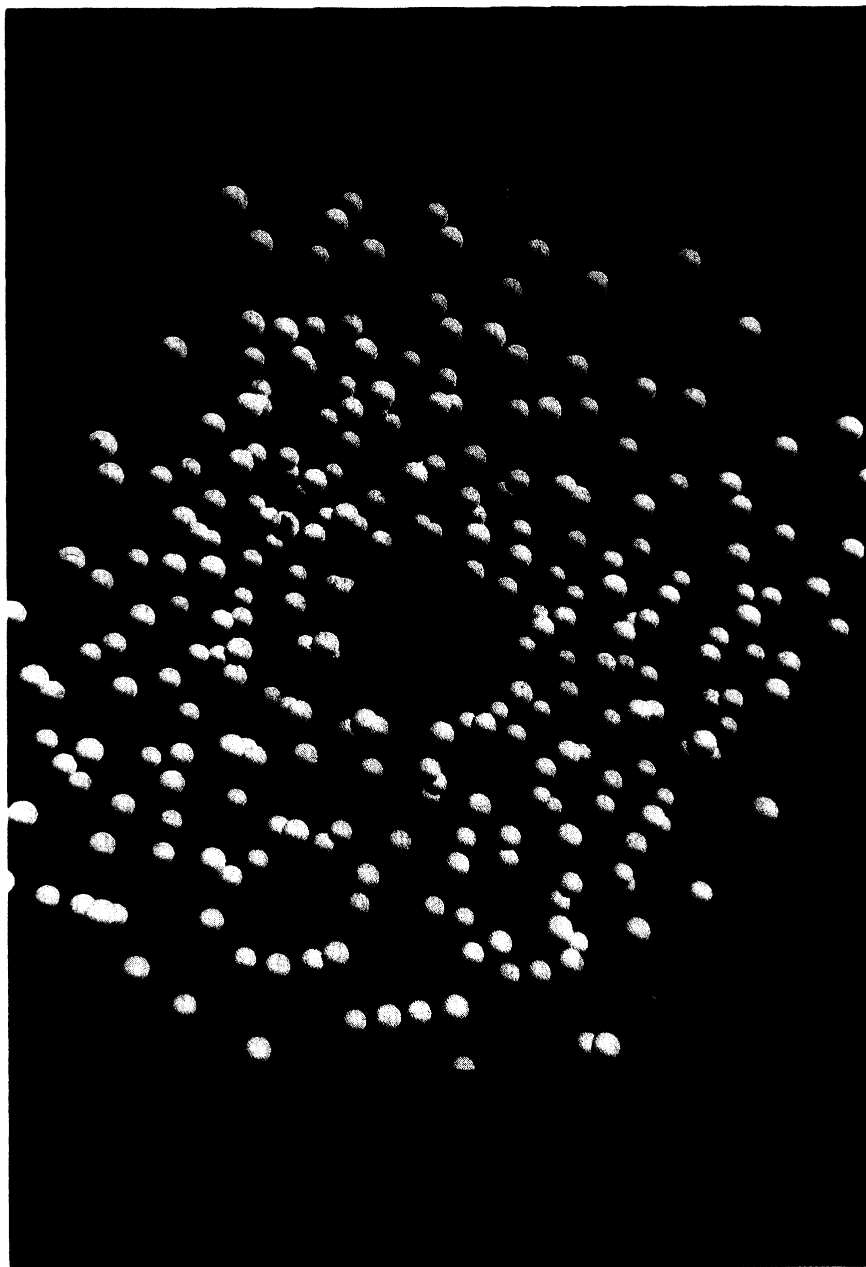

FIG. 1. A snapshot of electron density (red) and the positions of Si atoms (white).

IV. CALCULATIONS

The simulated systems consisted of 486 silicon atoms in a $41.05\times15.39\times15.39$Å^3 MD cell, so that the density in these simulations corresponded to the experimental density, $\rho=5\times10^{22}$ cm^{-3}, of the amorphous system. The electron wave function was represented on $64\times16\times16$ discrete grid points. Simulations with $128\times32\times32$ grid points were also performed to ascertain that the grid size had no effect on the results. The discrete time propagation of the electron wave packet was carried out with a time step, $\Delta t=1$ a.u. (0.024 fs), while the time step in the integration of Newton's equations for silicon atoms was 25 Δt. Periodic boundary condition was imposed.

Simulations were initiated by thermalizing the Si system without the excess electron at high temperature, $T=5000$ K. This well-thermalized system was cooled to a lower temperature and thermalized for a long time. With repeated cooling and thermalization, the system temperature was brought down to 300 K. At this stage a conjugate-gradient method was applied to the Si-atom configuration to bring the system to a local energy minimum. The excess electron was added to the Si system and its wave packet was propagated in imaginary time, using Eq. (4), until the electron reached the ground state corresponding to the given configuration of Si atoms. Next, in the presence of the excess electron, the Si atoms were relaxed to the minimum-energy configuration by the conjugate-gradient method. The imaginary-time propagation of the electron wave packet

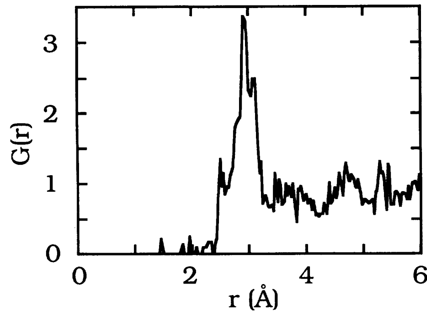

FIG. 2. Electron-silicon pair distribution function $G(r)$ calculated relative to the center of mass of the electron wave packet at $T=300$ K.

followed by the application of the conjugate-gradient method to the Si configuration were repeated until the combined excess electron and Si-atom system reached the lowest-energy configuration. Starting with this fully relaxed system, the electron wave packet was propagated in real time and the equations of motion for Si atoms were solved concurrently to obtain well-thermalized systems at temperatures $T=300$, 200, and 150 K. At each temperature the combined system was thermalized for at least 0.24 ps while the simulation proper was run for an additional 0.6 ps.

V. RESULTS

In the temperature range of 150–300 K, the excess electron is observed to be localized for the entire duration of the simulation. Figure 1 shows a typical snapshot of the excess electron and silicon atoms in the system at $T=300$ K. It is evident that the electron is trapped inside a void, around which the local tetrahedral arrangement of silicon atoms is destroyed. The snapshot in Fig. 1 indicates that the localized electron cloud is nearly spherical in shape. To assess the shape of the electron wave packet, we calculate a shape order parameter g from the radius of gyration tensor T: $\gamma=0.5[3\,\mathrm{Tr}(\mathrm{T}^2)/(\mathrm{Tr}\mathrm{T})^2-1]$, where $\mathrm{T}=\int d\mathbf{r}\,\mathbf{r}\,\mathbf{r}|\psi(\mathbf{r},t)|^2$. γ vanishes for a perfectly spherical wave packet, whereas for an infinitely elongated wave packet g is unity. The QMD simulations reveal that γ for the localized electron in the a-Si system is small (≤ 0.05) and remains so throughout the simulations at 300, 200, and 150 K.

An estimate for the size of the void trapping the electron can be obtained from the excess electron-silicon radial distribution function $G(r)$. Figure 2 shows such a distribution function measured relative to the center of mass of the electron wave packet. From the first peak in $G(r)$ we estimate that the size of the void is ~3 Å, and from the area under the first peak in $G(r)$ we find that the number of nearest-neighbor Si atoms is eight.

At temperatures between 150 and 300 K, nonequilibrium QMD simulations in the presence of a small external electric field were also performed to calculate the excess electron mobility. The mobility simulations were performed in the presence of a uniform external electric field of strength 1.03 V/cm in the x direction. Figure 3 shows the time variation of the velocity response at temperatures $T=300$, 200, and 150 K. From the ratio of the asymptotic values of the velocity response in the direction of the field and the field strength, we find that the excess electron mobility μ is (0.55 ± 0.20), (0.067 ± 0.012), and (0.007 ± 0.016) $\mathrm{cm^2/V\,s}$ at 300, 200, and 150 K, respectively. A comparison between the simulation results and the TOF mobility measurements[25] is shown in Fig. 4.[26] The simulation results for mobility exhibit a thermally activated behavior, just as experiments do. Fitting the simulation results to the formula for mobility to the multiple-trapping formula [Eq. (1)], we get the activation energy $\Delta E=(0.12\pm0.03)$ eV. The calculated activation energy compares well with the experimental value, 0.14 eV.[25] The same fitting gives the extended-state mobility $\mu_{\mathrm{ext}}=4$ $\mathrm{cm^2/V\,s}$ and the density-of-states ratio $g(E_c)/g(E_a)=13$. They also compare favorably with the corresponding experimental values 7.3 $\mathrm{cm^2/V\,s}$ and 30, respectively.[25] We have also calculated the velocity response of the electron using a time-dependent first-

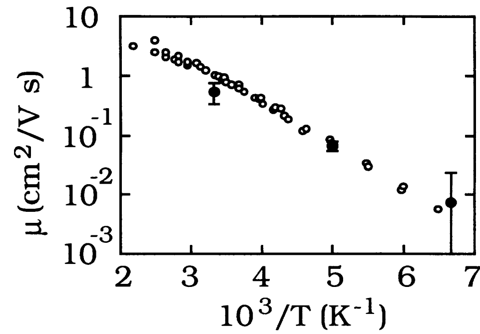

FIG. 3. Velocity response of an excess electron in a-Si in the presence of a uniform electric field of strength 1.03 V/cm. Velocities in the x, y, and z directions are denoted by solid, dashed, and dotted curves, respectively.

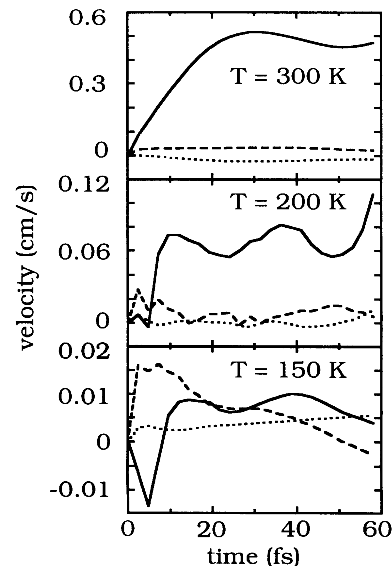

FIG. 4. Temperature dependence of the mobility of an excess electron in a-Si. Solid circles represent the QMD results. Open circles are the time-of-flight experimental results by Hourd and Spear (Ref. 25).

order perturbation method.[27] The results are identical to those obtained by the subtraction method. Thus an electric field of strength 1.03 V/cm corresponds to the linear-response regime.[28]

The results for the excess electron mobility depend on the topology of the network glass and the nature of defects trapping the electron. In the earlier TOF experiments, the room-temperature mobility was measured to be 0.1 $cm^2/V\,s$ and the activation energy over the temperature range of 150–300 K was 0.2 eV. More recent measurements find that the room-temperature mobility is 1 $cm^2/V\,s$ and the activation energy is 0.14 eV over the same temperature range. The observed differences between these experiments arise from different preparation conditions and, perhaps, the purity of samples. To test the effect of the former, we have performed mobility simulations using another set of initial conditions. In this case the simulation result for the room-temperature mobility, $\mu=(0.085\pm0.012)$ $cm^2/V\,s$, is much smaller than the value obtained from the previous simulations. To get an estimate of the activation energy, we have used the multiple-trapping model where the activation energy is the energy difference between the localized and extended states. Taking the difference between the ground and the first excited states to be a rough estimate of the activation energy, we find that its value for the second set of initial conditions is 0.2 eV. This agrees better with the earlier TOF measurements.

In conclusion, QMD simulations for an excess electron in *a*-Si reveal that defects such as voids tend to localize excess electrons. The size of these voids is ~3 Å. The mobility simulations between 150 and 300 K are in good agreement with the experimental results. Applying the multiple-trapping model to the simulation results, the values for the activation energy and the density-of-states ratio are in good agreement with the corresponding experimental values.

ACKNOWLEDGMENTS

This research was supported in part by the Louisiana Education Quality Support Fund, Grant No. LEQSF-(1991-1992)-RD-A-05, and National Science Foundation Grant No. ASC-9109906.

[1]J. M. Marshall, Rep. Prog. Phys. **46**, 1235 (1983).

[2]T. Tiedje, in *Semiconductors and Semimetals,* Vol. 21C, edited by J. Pankove (Academic, New York, 1984).

[3]W. E. Spear, J. Non-Cryst. Solids **90**, 171 (1987).

[4]J. M. Marshall, P. G. Le Comber, and W. E. Spear, Solid State Commun. **54**, 11 (1985).

[5]Reliable measurements become difficult near 150 K, although below 80 K the experimental results are reliable again. Starting around 80 K the electron mobility is observed to rise first with a decrease in the temperature and then saturate in the temperature range of 10–50 K. Furthermore, unlike the measurements between 150 and 320 K, the low-tempearture mobility data exhibit a dependence on the intensity of the excitation used for photogeneration of carriers.

[6]P. G. Le Comber and W. E. Spear, Phys. Rev. Lett. **25**, 509 (1970).

[7]A. I. Rudenko and V. I. Arkhipov, Philos. Mag. **39**, 465 (1979).

[8]T. Tiedje and A. Rose, Solid State Commun. **37**, 49 (1980).

[9]J. Orenstein and M. Kastner, Phys. Rev. Lett. **46**, 1421 (1981).

[10]E. A. Schiff, R. I. Devlin, H. T. Grahn, J. Tauc, and S. Guha, Appl. Phys. Lett. **54**, 1911 (1989).

[11]A. Selloni, P. Carnevali, R. Car, and Parrinello, Phys. Rev. Lett. **59**, 823 (1987).

[12]R. N. Barnett, U. Landman, and A. Nitzan, Phys. Rev. Lett. **62**, 106 (1989).

[13]R. K. Kalia and J. Harris, Solid State Commun. **73**, 839 (1990); R. K. Kalia, P. Vashishta, L. H. Yang, F. W. Dech, and J. Rowlan, Int. J. Supercomput. Appl. **4**, 22 (1990).

[14]R. K. Kalia, P. Vashishta, and S. W. de Leeuw, J. Chem. Phys. **90**, 6802 (1989).

[15]R. N. Barnett, U. Landman, and A. Nitzan (unpublished).

[16]G. Ciccotti and G. Jacucci, Phys. Rev. Lett. **35**, 789 (1975).

[17]A. Nakano, P. Vashishta, and R. K. Kalia, Phys. Rev. B **43**, 10 928 (1991).

[18]F. H. Stillinger and T. A. Weber, Phys. Rev. B **31**, 5262 (1985).

[19]W. D. Luedtke and U. Landman, Phys. Rev. B **40**, 1164 (1989).

[20]P. Hohenberg and W. Kohn, Phys. Rev. **136**, B864 (1964); W. Kohn and L. J. Sham, *ibid.* **140**, A1133 (1965).

[21]W. Y. Ching, C. C. Lin, and L. Guttman, Phys. Rev. B **16**, 5488 (1977).

[22]G. B. Bachelet, D. R. Hamann, and M. Schlüter, Phys. Rev. B **26**, 4199 (1982).

[23]J. Perdew and A. Zunger, Phys. Rev. B **23**, 5048 (1981).

[24]D. M. Ceperley and B. J. Alder, Phys. Rev. Lett. **45**, 566 (1980).

[25]A. C. Hourd and W. E. Spear, Philos. Mag. B **51**, L13 (1985).

[26]At 150 K the drift velocity becomes so small that it is masked by thermal fluctuations, resulting in a large error bar in the calculated mobility. This causes large uncertainties in the calculated extended-state mobility and the density-of-state ratio. A much longer simulation will improve the accuracy.

[27]For classical systems, calculation of response by the first-order perturbation theory is described by G. Ciccotti, G. Jacucci, and I. R. McDonald, J. Stat. Phys. **21**, 199 (1979). The present method is an extension of their method to mixed quantum and classical systems.

[28]In neither equilibrium nor nonequilibrium simulations did we find any deviations from adiabaticity in the electron dynamics. At regular time intervals, the real-time QMD simulations were interrupted, the silicon atoms were held fixed, and the electron wave packet was propagated in imaginary time. The imaginary-time propagation causes the electron to reach the ground state corresponding to the fixed configuration of silicon atoms. Next the overlap of this ground-state electron wave function with the initial wave function was calculated. At all times the overlap was very close to unity.

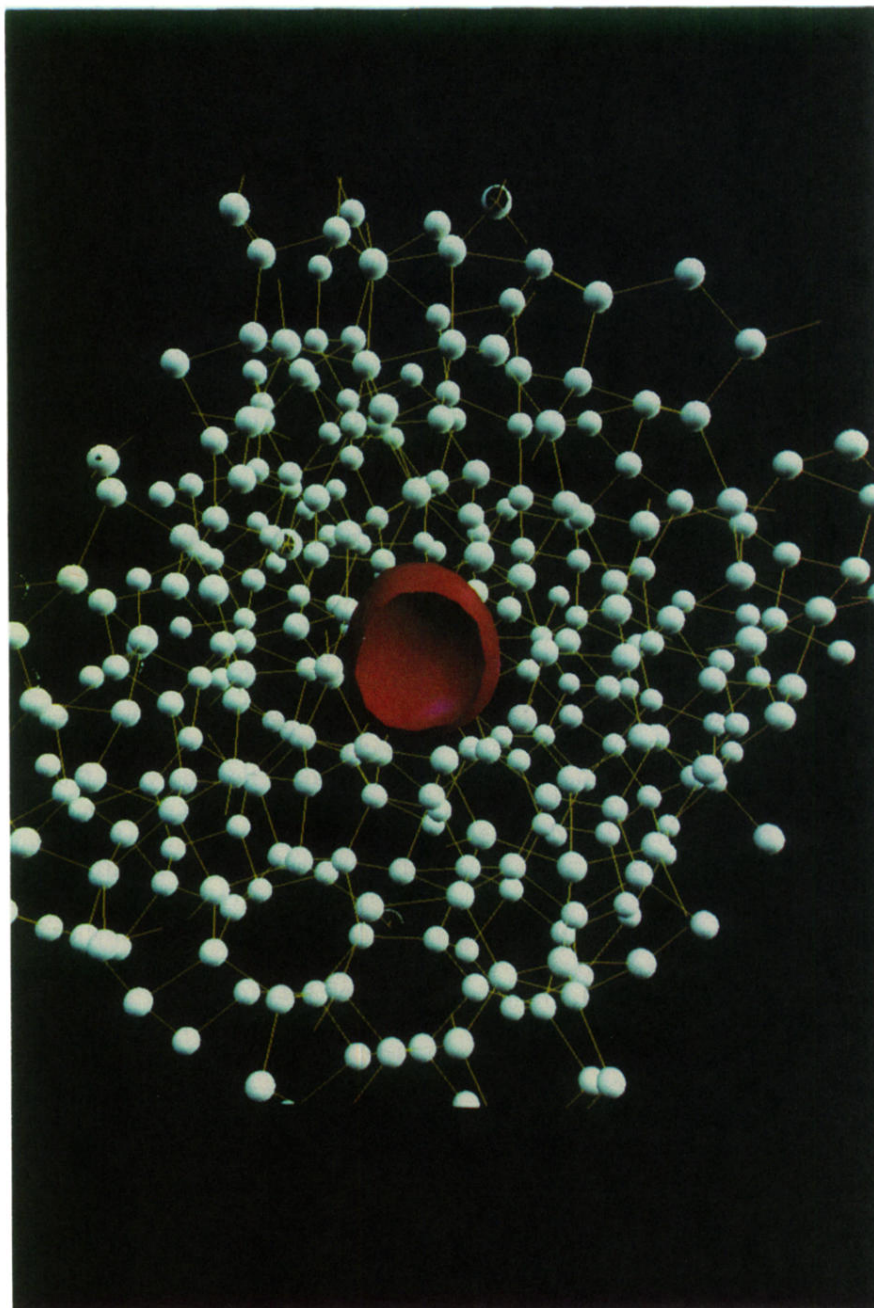

FIG. 1. A snapshot of electron density (red) and the positions of Si atoms (white).